Eur. Phys. J. C 49, 365–369 (2007)
DOI 10.1140/epjc/s10052-006-0112-7

THE EUROPEAN PHYSICAL JOURNAL C

Regular Article – Experimental Physics

J/ψ production in PHENIX

R. Granier de Cassagnac[a] for the PHENIX Collaboration

Laboratoire Leprince-Ringuet, École polytechnique/IN2P3, 91128 Palaiseau, France

Received: 11 August 2006 /
Published online: 16 November 2006 –

Abstract. Heavy quarkonia production is expected to be sensitive to the formation of a quark gluon plasma (QGP). The PHENIX experiment has measured J/ψ production at $\sqrt{s_{NN}} = 200$ GeV in Au + Au and Cu + Cu collisions, as well as in reference $p+p$ and $d+$Au runs. J/ψ's were measured both at mid ($|y| < 0.35$) and forward ($1.2 < |y| < 2.2$) rapidity. In this letter, we present the $A+A$ preliminary results and compare them to normal cold nuclear matter expectations derived from PHENIX $d+$Au and $p+p$ measurements as well as to theoretical models including various effects (color screening, recombination, sequential melting...).

1 Introduction

PHENIX is one of the experiments located at the relativistic heavy ion collider (RHIC) of Brookhaven National Laboratory. It has the capability of measuring quarkonia through their dilepton decay in four spectrometers: two central arms covering the mid-rapidity region of $|\eta| < 0.35$ and twice $\pi/2$ in azimuth, and two forward muon arms covering the full azimuth and $1.2 < |\eta| < 2.2$ in pseudo-rapidity. Electrons are identified in the central arms by their Čerenkov rings and by matching the momentum of charged particles reconstructed in drift chambers with the energy deposited in an electromagnetic calorimeter. In the forward arms, muons are selected by an absorber and identified by the depth they reach in a succession of proportional counters staggered with steel walls. The event vertex and centrality are measured by beam-beam counters situated at $3 < |\eta| < 3.9$. For $A+A$ collisions, the centrality measurement is further refined by the use of two zero degree calorimeters located downstream the beams. A detailed description of the PHENIX apparatus can be found in [1].

This letter is organized as follows: we first set up the references by looking at $d+$Au data (Sect. 2) and compare the cold nuclear matter effects derived from it to $A+A$ data (Sect. 3). In Sect. 4, we compare our results to what was observed at the CERN SPS. We then review in Sect. 5 the state of the art of the possible explanations of our observed suppression. Kinematic distributions could help distinguishing between models and we present our rapidity (Sect. 6) and mean squared transverse momentum (Sect. 7) before to conclude in Sect. 8.

Note that all $A+A$ J/ψ data shown below are PHENIX preliminary.

[a] e-mail: raphael@in2p3.fr

2 J/ψ production in $d+$Au collisions

The nuclear modification factor R_{AB} for any $A+B$ collision type is defined as the J/ψ yield observed in these collisions, divided by the yield measured in a $p+p$ run and scaled by the average number of nucleon–nucleon collisions $\langle N_{\rm coll}\rangle$ extracted from a Glauber model:

$$R_{AB} = \frac{\mathrm{d}N_{AB}^{J/\psi}}{\langle N_{\rm coll}\rangle \, \mathrm{d}N_{pp}^{J/\psi}} \quad (1)$$

Departure from $R_{AB} = 1$ implies some nuclear modifications of the produced J/ψ's. The PHENIX collaboration has measured the J/ψ nuclear modification factor for $d+$Au collisions [2]. Its centrality dependence is shown on Fig. 1 for our three rapidity ranges.

In $d+$Au collisions at 200 GeV, J/ψ's in our three rapidity ranges probe the following momentum fractions x of gluons in the gold nucleus (neglecting the emitted gluon): 0.05 to 0.14 (upper panel, negative rapidity, gold-going side), 0.011 to 0.022 (midrapidity) and 0.0014 to 0.0047 (lower panel, positive rapidity, deuteron-going side). The difference observed between forward (lower panel) and backward (upper panel) yields indicate that shadowing and/or anti-shadowing are at play. These effects are modifications of the parton distribution functions in nuclei with respect to the usual functions in free nucleons. In particular, one expect a depletion (shadowing) at low x due to overlapping and recombining partons (gluons in the case of J/ψ). The strength of gluon shadowing is not heavily constrained by theory and models predictions [3–5] differ by a factor of three.

Comparison with Vogt's theoretical predictions [6] shows that a modest amount of absorption (0 to 3 mb), added to a modest amount of shadowing such as the

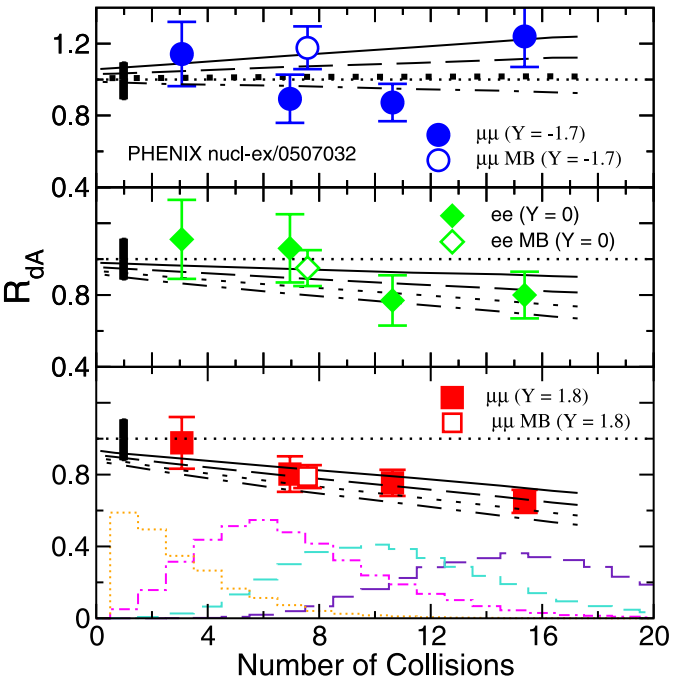

Fig. 1. J/ψ nuclear modification factor R_{dA} as a function of centrality (given here by the number of collisions $N_{\rm coll}$) for backward (*top*, $y=-1.7$) mid (*middle*, $y=0$) and forward (*bottom*, $y=1.8$) rapidities. The *histograms* are the distributions of $N_{\rm coll}$ for each of our four centrality classes. Theoretical curves are from Vogt [6] and take EKS shadowing and 0, 1, 2 or 3 mb normal absorption cross section (from *top solid* to *bottom dot-dashed*)

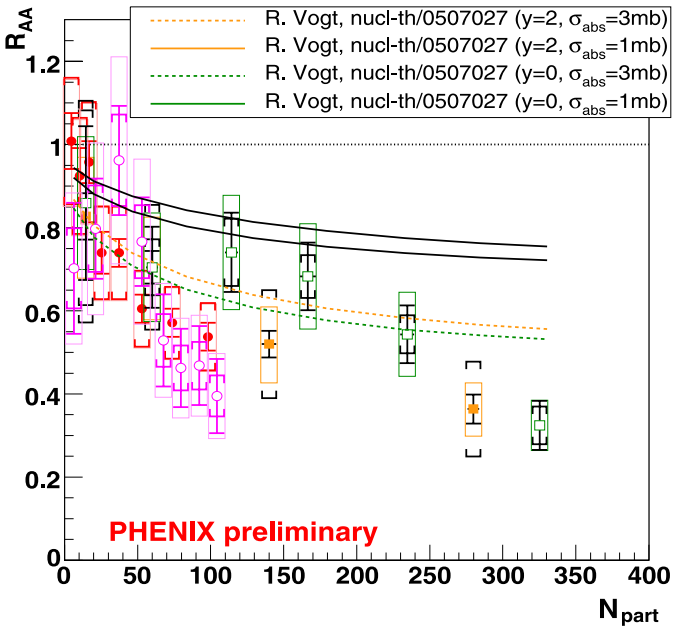

Fig. 2. Nuclear modification factor R_{AA} as a function of centrality (given here by the number of participants $N_{\rm part}$) for Cu + Cu $y=0$ (*open circles*) Cu + Cu $y=1.7$ (*full circles*) Au + Au $y=0$ (*open squares*) and Au + Au $y=1.7$ (*full squares*). Error bars are statistical, brackets are systematics, and box are global (common to all the points). Theoretical curves are Au + Au cold nuclear effects only predictions from Vogt [8], *solid* and *dashed lines* being for 1 mb and 3 mb normal nuclear absorption cross sections, respectively

one provided by the Eskola–Kolhinen–Salgado (EKS [3]) scheme, can describe both the rapidity and centrality dependencies, as shown on Fig. 1.

3 Normal nuclear matter effects in $A+A$

To extrapolate the effects seen in $d+$Au to $A+A$ collisions, one has to rely on a model. Together with our Au + Au ($\sim 0.2\,{\rm nb}^{-1}$) and Cu + Cu ($\sim 3\,{\rm nb}^{-1}$) measurements [7], Au + Au predictions from such a cold nuclear matter model [8] are presented on Fig. 2, as a function of centrality (displayed here as the number of participants). They account for shadowing (following the EKS prescription) and nuclear absorption (1 mb for solid lines and 3 mb for dashed lines). Predictions are shown for two rapidity values ($y=0$ and $y=2$) corresponding to our two rapidity regions. The difference between the 1 mb and the 3 mb curves gives an idea of our current uncertainty on the cold nuclear matter effects affecting the J/ψ production in $A+A$ collisions.

However, in both rapidity ranges, our most central Au + Au measurements depart from the predictions made with the stronger nuclear effects (3 mb), suggesting that other suppression mechanisms are involved, namely, an anomalous suppression.

4 Lower energy anomalous suppression

Such an anomalous suppression was early predicted by Matsui and Satz as a signature of the QGP [9] and later observed by the CERN NA50 experiment [10] at lower energy ($\sqrt{s_{NN}}=17.3\,{\rm GeV}$). Various models explain the NA50 data and the extrapolation of three of them to RHIC energies are displayed on Fig. 3 together with our Au + Au data.

In [11] (solid lines), J/ψ's are absorbed by comoving particles (of undetermined partonic/hadronic nature). In [12], the authors describe the dynamical interplay between suppression and regeneration of J/ψ's in a QGP. The suppression mechanism is dominant for NA50 energies and is the only one presented here (see Fig. 4 for the full prediction). In [13] (dot-dashed lines), the authors use a QGP statistical charm coalescence model. All three models fail to reproduce our data, overestimating the measured suppression. Other models such as percolation [14] also overpredict the suppression, suggesting that new mechanisms are at play at RHIC energy.

5 Alternate explanations for suppression

For now, at least three classes of models exist that can roughly accommodate the amount of anomalous suppres-

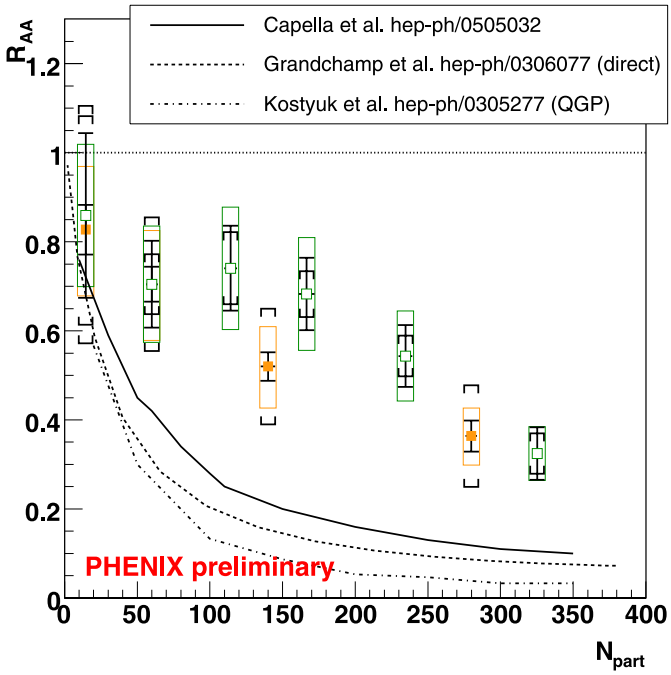

Fig. 3. Nuclear modification factor R_{AA} as already presented on Fig. 2. Only Au + Au data are shown ($y = 0$ *open symbols*, $y = 1.7$ *full symbols*). Theoretical curves are predictions from models that describe the anomalous suppression seen by the NA50 experiment at lower energies [11–13]

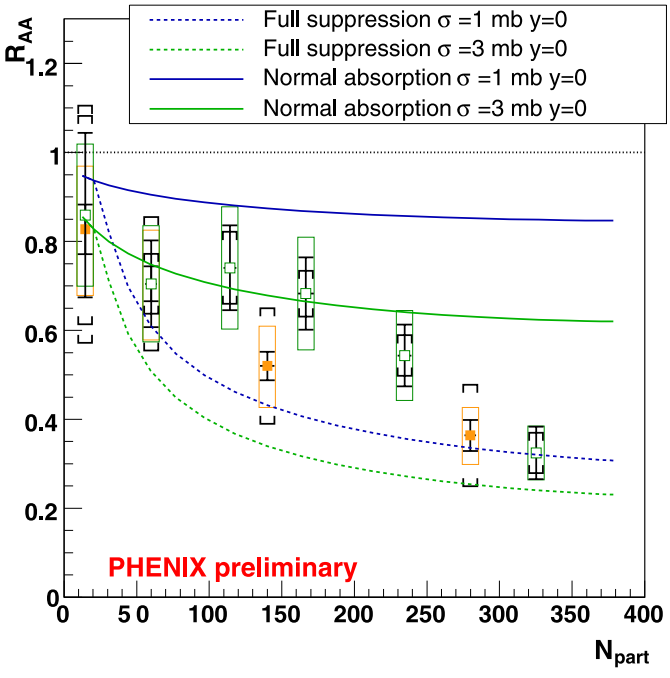

Fig. 4. Nuclear modification factor R_{AA} as already presented on Fig. 2. Only Au + Au data are shown ($y = 0$ *open symbols*, $y = 1.7$ *full symbols*). Theoretical curves are from a J/ψ transport model in an hydrodynamical quark gluon plasma [15]. The *dashed* (*solid*) *lines* are with (without) anomalous suppression. The *up (down) curves* are with 1 mb (3 mb) normal nuclear absorption

sion seen in our most central preliminary results. The accuracy of the present data, as well as the uncertainty on the cold nuclear effects, do not allow to favor one or the other. We review them in the three following subsections.

5.1 Detailed transport

One paper [15], simulating J/ψ transport in a hydrodynamical model, actually predicts an amount of suppression that matches our most central data. It is shown on Fig. 4 where the authors have added cold nuclear matter effects (nuclear absorption only, 1 or 3 mb) with respect to the published paper. The suppression they obtain is not large because they authorize J/ψ's with sufficient momenta to freely stream out of the plasma.

5.2 Sequential melting

An important fraction (30 to 40%) of J/ψ's comes from feed-down decays of charmonia excited states (ψ', χ_c). This particular point is taken care of in most of the previous approaches. But recent lattice computations indicate that J/ψ's could melt at a much higher temperature than the one that was originally thought. One possible hypothesis, defended in [16], is that only the excited states melt, leaving all the initially produced J/ψ's untouched. This 30 to 40% suppression could also match our data.

5.3 Recombination

At RHIC energies, multiple $c\overline{c}$ pairs are produced (10 to 20 in central collisions according to [17]). Quark mobility in a deconfined medium could allow uncorrelated charm quarks to recombine when the QGP fireball freezes, forming quarkonia, and raising their yield with centrality. A balance between suppression and enhancement could lead to the intermediate suppression we observe. Figure 5 shows a collection of predictions from various recombination or coalescence models, from [12, 18–20]. Unfortunately, the lack of knowledge of the yield and distributions of charm quarks initially produced as well as of the recombination mechanism, make these predictions hardly predictive. A good way to search for hints of recombination is then to look at its impact on the distributions of kinematical quantities, such as rapidity and transverse momenta.

6 J/ψ rapidity profile

According to [20], the rapidity distribution of the recombined J/ψ's should be modified with respect to the directly produced J/ψ's. In particular, it should emphasize the region of phase space where more c quarks are produced, because recombination probability goes quadratically with the c quark densities. Recombined J/ψ's should then have a narrower rapidity distribution. Figure 6 shows our measured rapidity spectra for three Au + Au and four Cu + Cu centrality classes, as well as for $p + p$.

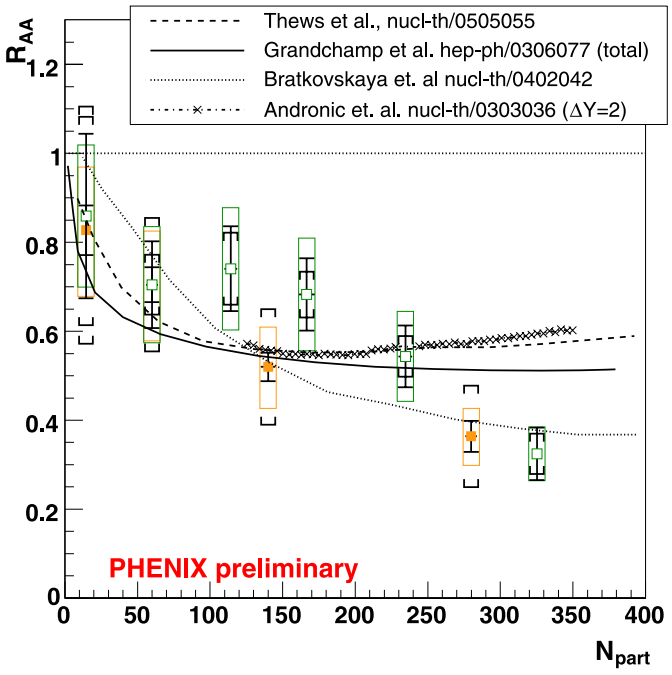

Fig. 5. Nuclear modification factor R_{AA} as already presented on Fig. 2. Only Au + Au data are shown ($y = 0$ *open symbols*, $y = 1.7$ *full symbols*). Theoretical curves come from various recombination models (*solid* [12], *dotted* [18], *crossed* [19] and *dashed* [20])

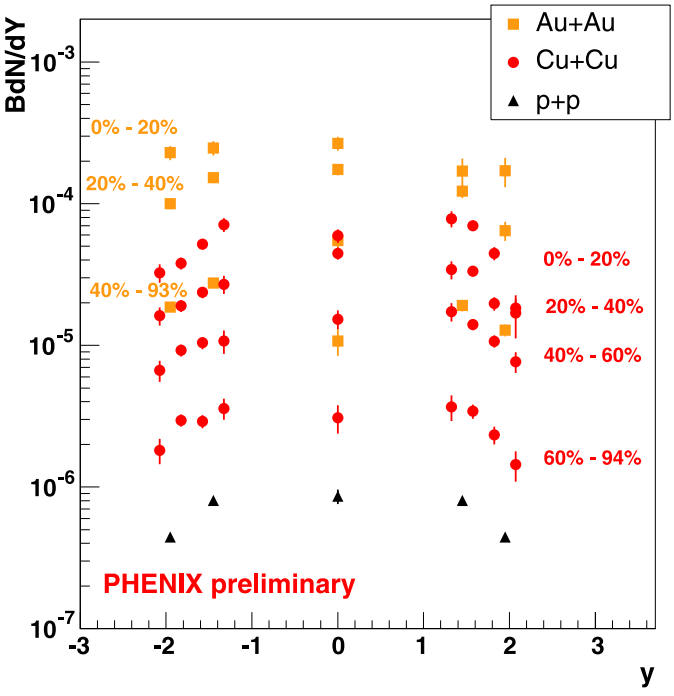

Fig. 6. J/ψ rapidity spectra for three Au + Au centrality intervals (*squares*), four Cu + Cu centrality intervals (*circles*) and $p + p$ collisions (*triangles*)

Within our limited statistical accuracy, we do not see any modification of the rapidity profile and cannot draw any conclusion towards or against recombination from this.

7 J/ψ mean transverse momentum

Recombination modifies transverse momentum as well. Figure 7 shows our measured mean squared transverse momentum $\langle p_{\mathrm{T}}^2 \rangle$ for various systems and centrality intervals, as a function of N_{coll}. The shaded bands are predictions from [20], corresponding to either J/ψ's from recombination (lower band) or to directly produced J/ψ's (upper band). To properly predict the modified p_{T} spectra, one first needs to quantify the normal p_{T} broadening coming from cold nuclear effects (Cronin effect). This effect was clearly seen by PHENIX [2] at forward rapidity, by comparing $\langle p_{\mathrm{T}}^2 \rangle$ in $p + p$ and $d + \mathrm{Au}$ collisions. In [20] the authors use these measurements to quantify the Cronin effect. However, at midrapidity, because of the very poor statistics of the $p + p$ sample, it is difficult to quantify it. Thus, the theoretical prediction can only be safely compared to the forward rapidity case.

The solid line is another parametrization of the Cronin effect from [21], using this simple parametrization:

$$\langle p_{\mathrm{T}}^2 \rangle_{AA} = \langle p_{\mathrm{T}}^2 \rangle_{pp} + \rho\sigma\delta(\langle p_{\mathrm{T}}^2 \rangle) \times L = 2.51 + 0.32 \times L\,, \quad (2)$$

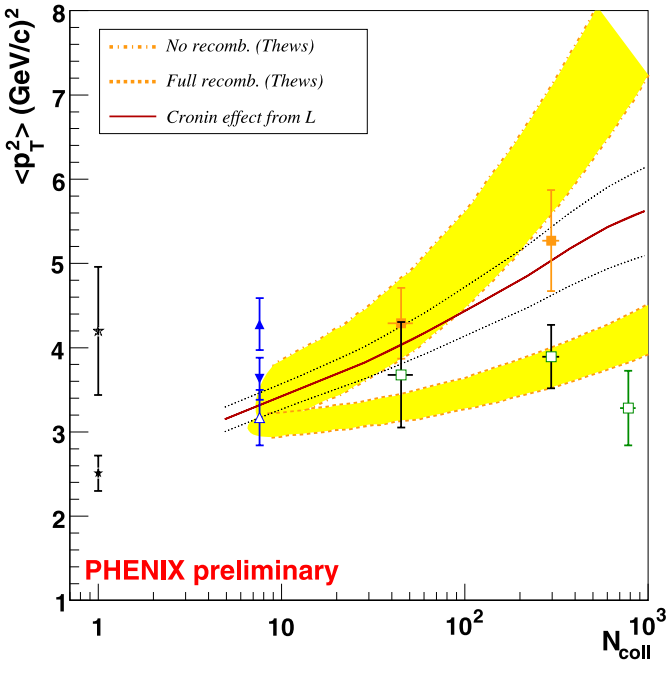

Fig. 7. Mean squared transverse momentum versus N_{coll}. *Black stars* at $N_{\mathrm{coll}} = 1$ are for $p + p$ collisions, for mid (*upper*) and forward (*lower*) rapidity. *Triangles* are for $d + \mathrm{Au}$, for mid (*open*) and forward/backward (*full*) rapidity. *Squares* are for Au + Au for mid (*open*) and forward (*full*) rapidity. Shaded bands are from [20] and stands for direct (*lower band*) or fully recombined J/ψ's (*upper band*). The *solid line* is a parametrization of Cronin effect derived from $d + \mathrm{Au}$ data in [21], the *dotted lines* on each side reflecting the associated errors

where $\langle p_{\mathrm{T}}^2 \rangle$ is in units of $(\mathrm{GeV}/c)^2$ and L is, in fermis, the average thickness of nuclear matter seen by a J/ψ in the collision system and the centrality bin considered. The factor $\rho\sigma\delta\left(\langle p_{\mathrm{T}}^2 \rangle\right) = 0.32$ is determined by the $d+\mathrm{Au}$ forward data and stands for the nuclear density ρ, times the elastic gluon–nucleon scattering cross section σ, times the average p_{T} kick given at each scattering $\delta(\langle p_{\mathrm{T}}^2 \rangle)$. The dotted lines on each side of the main curve are the errors derived from the $p+p$ and $d+\mathrm{Au}$ uncertainties. This parametrization provided a good description of lower energy experiments [21] and matches our data when it can be safely applied, namely at forward rapidity.

Thus, the raise of $\langle p_{\mathrm{T}}^2 \rangle$ at forward rapidity in Au+Au collisions seems explainable by the Cronin effect only. A better $p+p$ baseline is needed to interpret the rather centrality independent $\langle p_{\mathrm{T}}^2 \rangle$ we observe at midrapidity.

8 Conclusions

PHENIX preliminary results show a substantial amount of J/ψ suppression, growing with centrality. At the highest energy density probed so far, this suppression is as large as a factor of three. However, its interpretation is not easy. First, the amount of normal, cold nuclear matter suppression is not precisely known and demands more $d+A$ data. Nevertheless, the observed suppression in $A+A$ seems to exceed the maximum suppression authorized by cold nuclear matter, and thus be partly anomalous.

It also seems weaker than the suppression derived from models that fit lower energy data. Three classes of models that raise the number of surviving J/ψ's were presented. They all suppose the formation of a QGP. To distinguish between them, a better precision on data, and in particular on the kinematical distributions, is required.

References

1. PHENIX Collaboration, Nucl. Instrum. Methods A **499**, 469 (2003)
2. PHENIX Collaboration, Phys. Rev. Lett. **96**, 012 304 (2006)
3. K.J. Eskola, V.J. Kolhinen, C.A. Salgado, Eur. Phys. J. C **9**, 61 (1999)
4. L. Frankfurt, M. Strikman, Eur. Phys. J. A **5**, 293 (1999)
5. B.Z. Kopeliovich et al., Phys. Rev. C **72**, 054 606 (2005)
6. R. Klein, R. Vogt, Phys. Rev. Lett. **91**, 142 301 (2003)
7. PHENIX Collaboration, H. Pereira da Costa, Nucl. Phys. A **774**, 747 (2006) [nucl-ex/0510 051]
8. R. Vogt, nucl-th/0507027 and private communications
9. T. Matsui, H. Satz, Phys. Lett. B **178**, 416 (1986)
10. NA50 Collaboration, Eur. Phys. J. C **39**, 335 (2005)
11. A. Capella, E.G. Ferreiro, Eur. Phys. J. C **42**, 419 (2005) (and private communications)
12. L. Grandchamp et al., Phys. Rev. Lett. **92**, 212 301 (2004) (and private communications)
13. A.P. Kostyuk et al., Phys. Rev. C **68**, 041 902 (2003)
14. S. Digal et al., Eur. Phys. J. C **32**, 547 (2004)
15. X.L. Zhu et al., Phys. Lett. B **607**, 107 (2005) (and private communications)
16. F. Karsch et al., Phys. Lett. B **637**, 75 (2006)
17. PHENIX Collaboration, Phys. Rev. Lett. **94**, 082 301 (2005)
18. E.L. Bratkovskaya et al., Phys. Rev. C **69**, 054 903 (2004) (and private communications)
19. A. Andronic et al., Phys. Lett. B **571**, 36 (2003) (and private communications)
20. R.L. Thews, M.L. Mangano, Phys. Rev. C **73**, 014904 (2006) (and private communications)
21. V.N. Tram, PhD thesis, École polytechnique and nucl-ex/0606017